YEAR 3 GEOLOGIC MAPPING OF CENTRAL VALLES MARINERIS, MARS. C. M. Fortezzo[1], A. L. Gullikson[1], J. A. P. Rodriguez[2], T. Platz[2,3], and P. S. Kumar[4]; [1]U.S. Geologic Survey, Astrogeology Science Center, 2255 N. Gemini Dr., Flagstaff, Arizona 86001 (cfortezzo@usgs.gov); [2]Planetary Science Institute, Tucson, AZ; [3]Max Plank Institute for Solar System Research, Göttingen, Germany; [4]National Geophysical Research Institute, Hyderabad, India.

Introduction: Valles Marineris (VM) constitutes the largest canyon system in the Solar System and has a complex history. It consists of interconnected and enclosed troughs that extend from the Tharsis volcanic complex to the southern circum-Chryse outflow channels [1]. The central portion of VM (CVM, Fig. 1) includes the deepest of these troughs.

Within the CVM troughs occur the thickest exposed sections of (a) layered wall rocks on Mars, mostly lavas and other early crustal rocks [2-3], and (b) interior layered deposits (ILD), generally thought to be of sedimentary or volcanic origin [4]. The trough floors are extensively covered by landslides, fans, and eolian deposits. In addition, they appear locally dissected by channel networks and include patches of fractured terrain development.

The plateau surfaces that surround the troughs are extensively cratered and modified by contraction (wrinkle) ridges and extensional faults and grabens, some of which are aligned with pit chains. The plateau surfaces are covered by various types of flow deposits including some of possible volcanic and sedimentary origin.

Methodology: Using geographic information system (GIS) software, we are characterizing and mapping the distribution of materials and features exposed within the canyons and on the plateaus surrounding CVM at 1:1,000,000-scale. Recommended mapping methodologies for this scale, call for drafting at 1:250,000-scale using a linear vertex spacing of 500 m. We are examining the timing relationships among unit outcrops and features through mapping (i.e., unit contacts, marker beds, and unconformities) and crater densities. For the latter, we are using CraterTools [7], a GIS add-on, to count craters on discrete geologic materials, and CraterStats [8] to plot ages [e.g., 9]. We used LayerTools [10] to investigate if we could accurately measure bedding orientations of the interior layered deposits (ILD). We are using CRISM-CAT in IDL/ENVI to examine the CRISM spectra.

Datasets: The Mars Reconnaissance Orbiter (MRO) Context Camera (CTX) mosaic provides ~95% coverage over the map area, with 99% coverage within the troughs, at 6 m/pix. The Mars Express High-Resolution Stereo Camera (HRSC) provides both visible-range at 12.5 - 25 m/pix and topography at 50 m/pix. Mars Odyssey THEMIS daytime and nighttime infrared controlled mosaics [11] provide details at 100 m/pix and will aid in determining material variation based on thermal differences. In addition, we also utilize Mars Global Surveyor MOLA data (460 m/pix), MRO HiRISE images (≥25 cm/pix), where supportive, and OMEGA and CRISM hyperspectral data, where applicable.

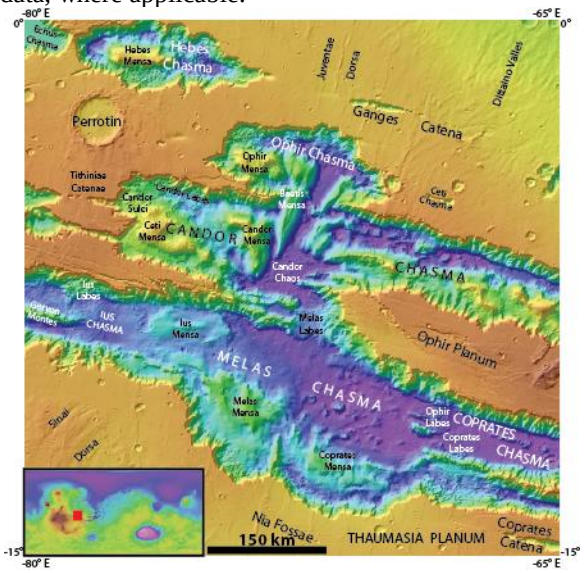

Figure 1: MOLA shaded relief (463 m/pix) overlying THEMIS daytime infrared mosaic (100 m/pix) of the mapping region (0° to 15°S, -80° to -65°E) with nomenclature.

CVM Mapping results: We have identified eight categories of material units, based on their typical geographical settings, geomorphic expressions, and geologic origins. Categories are made up of multiple map units, subdivided by additional morphology criteria, and by relative age. In addition, we are documenting further temporal relationships within units, including wall rock terraces and individual mass wasting lobes within overlapping sequences. Temporal inferences can be made based on (a) cross-cutting relationships among outcrops of the same unit separated by internal contacts and structures and on (b) dating of temporally related features such as landslide alcove development.

The unit groups consist of: (1) *Surficial materials* including low-albedo mantles, sand sheets, transverse aeolian ridge fields, and dunes; (2) *crater* and *ejecta materials*; (3) *mass wasting* typically proximal to canyon walls with geomorphology categorized using a terrestrial scheme [11]; (4) *catena materials*, including a floor and a wall unit, including incipient collapse features; (5) *chasma floor materials* consisting of eolian, smooth, blocks, massifs, channel and flood deposits,

and cavi exposures of subsurface materials; (6) *interior layered deposits* within VM troughs that include upper, middle, and lower units with locations to be further refined where possible; (7) *wall deposits* consisting of a gullied and smooth; and (8) *plateau materials* made up of three widespread plateau units, three fluvial terrace units, flow materials, and a highland massif unit.

We have divided the *mass wasting* materials into subgroups based on their geomorphology using the terrestrial classification scheme in [12]. We identified the following groups (subgroups in parentheses) in descending order of frequency: flows (debris, "earth", and solifluction), slides (rock planer, multiple rotation, single rotation, debris, translational debris, and successive rotational), falls (rock, "earth", and debris), spreads (debris and rock), and topples.

In addition, we are mapping linear features where useful in reconstructing the geologic history. These features include unit *contacts* with certain, approximate, buried, and internal younger/older relationship types. *Tectonic features* include inferred grabens, normal faults, and contractional wrinkle ridges. Some *ridges* are differentiated as sinuous (possible inverted fluvial features), curvilinear on landslides, and erosional geomorphologies (yardangs and massifs). *Scarps* are mapped at collapse margins, landslide heads and toes, and flow margins.

The tectonic feature mapping shows 5 generations of graben development preserved on the plateau and within the canyon walls: (1) oriented roughly NNE-SSW, mostly confined to Sinai Dorsa, surrounding an ancient caldera; (2) circumferential to the alcoves in southern Melas Chasma, possibly key to expansion of these alcoves; (3) oriented roughly NNE- SSW, paralleling most of the wrinkle ridges, located in Thaumasia and Lunae Plana, and in the Tithoniae Catenae region; (4) oriented WNW-ESE and paralleling and bounding the chasmata throughout the region, these graben are prevalent on Ophir Planum, may be responsible for canyon widening; (5) isolated to Ophir Planum, these are curvilinear faults expressions that may be reactivations of older structures.

Channels are mapped to show the influence fluvial processes in the development of CVM. Finally, we mapped *crater rim crests* and *buried crater* features larger than 5 km.

Crater Statistics: We have detailed crater counts on a selection of mass wasting units located in eastern Ius (1 age) and northern Melas Chasmata (3 ages), and on Ophir Planum (4 ages) and Coprates Labes (1 unit). These ages (Table 1) are younger than those reported in [13] by at least half. These data indicate that trough expansion through mass wasting processes have been important in the very recent history of CVM. For these counts, we used CTX data which should have similar resolutions to the Mars Obiter Camera used in [13] to perform and report crater statistics, but with expanded areal coverage.

Table 1: Ages from current and previously published work.

Location	Age (Ma)	Quantin ID	Quantin Age (Ma)
Coprates Labes	63	38	400
Ophir Labes	64-41	40 & 41	500-150
Ius Labes	412	25	>1000
Northern Melas	700-280	32 & 33	1000 - >1500

Detailed crater counts on the plateau units indicate Thaumasia and Lunae to have similar primary emplacement ages (~3.75-3.6Ga) with Ophir indicating a wider range of emplacement (~4.0-3.4Ga). The older age in Ophir Planum is associated with an interpreted ancient volcanic edifice and the younger age is associated with the faulted plateau units. Two resurfacing periods are indicated by the crater statistics. The first is 2.7Ga, 2.8–2.2Ga, and 1.9Ga and the second is geologically recent at 1.0Ga, 0.6-0.2Ga, and 1.3-1.0Ga in Thaumasia, Ophir, and Lunae Plana, respectively.

Interior Layered Deposits: In an effort to subdivide the units of the ILD in CVM, we used HRSC stereo and the CTX mosaic to determine bedding orientations using the LayerTools [10]. We tested whether the lower resolution, but areally extensive HRSC would garner similar results to bedding orientations on HiRISE-derived DTMs. We compared our results to [14], and found agreement in both the magnitude of dips and the dip directions. A significant problem is that all of our measured dip magnitudes were within the range of the slope in the measurement areas. We have determined this to be an unreliable method of gathering the bedding orientations, and subdividing the ILD. We are now considering morphologic variations in bedding, erosional character, and incorporating CRISM mineralogic data.

References: [1] Lucchitta B.K. et al. (1992) in Kieffer H.H. et al. (eds.) *Mars*, U. Arizona Press, p. 453-492. [2] McEwen A.S. et al., (1999) *Nature*, 397. [3] Murchie S.L. et al. (2010) *J. Geophys. Res.*, 114. [4] Lucchitta B.K. et al. (1994) *J. Geophys. Res.*, 99. [5] Witbeck N.E. et al. (1991) *USGS Map I-2010.* [6] Dohm J.M. et al. (2009) *J. Volcan. Geotherm. Res.*, 185. [7] Kneissl T. et al. (2010), *Planet. Space Sci.*, 59 (11-12). [8] Michael G.G. and Neukum G. (2010) *Earth Planet. Sci. Lett.*, 294. [9] Platz T., et al. (2013), *Icarus*, 225. [10] Kneissl T., et al. (2010) *LPSC*, Abst. #1640. [11] Fergason R.L. et al. (2013) *LPSC*, Abst. #1642. [12] Hungr, O. et al. (2014) *Landslides*, 11:167-194. [13] Quantin, C. et al. (2004) *Icarus*, 172 :555-572. [14] Okubo, C.H. (2014) *USGS Map SIM3309.*